

Sickle cell anemia in images from head-to-toe

Anemia de células falciformes en imágenes de la cabeza a los pies

María Isabel González Gómez[1]
Mónica Royero Arias[2]
Jorge Ochoa Gaviria[23]
Laura Moreno[4]
https://doi.org/10.53903/01212095.320

Summary

Sickle cell disease (SCD) is an autosomal recessive entity characterized by abnormal hemoglobin formation. The manifestations of SCD are mainly due to vaso-occlusive crises, hemolysis or infection and usually present with multisystem involvement. For the most part, clinical and imaging findings will suggest the diagnosis and allow adequate follow-up. Different diagnostic modalities such as ultrasound, computed tomography and magnetic resonance imaging play an essential role in identifying complications of SCD. Knowledge of the different specific radiological manifestations of the disease will allow us to make a correct differential diagnosis with other hematologic diseases, an adequate follow-up of this pathology and an early and timely treatment. With this article we intend to familiarize the radiologist with the SCD multisystemic spectrum in the pediatric population.

Key words (MeSH)

Anemia, sickle cell
Diagnostic imaging
Radiology
Pediatrics

Palabras clave (DeCS)

Anemia de células falciformes
Diagnóstico por imagen
Radiología
Pediatría

Resumen

La anemia de células falciformes (ACF) es una entidad autosómica recesiva caracterizada por la formación anormal de hemoglobina. Las manifestaciones de la ACF se deben principalmente a crisis vasoclusivas, hemólisis o infección; suele cursar con un compromiso multisistémico. En su mayoría, los hallazgos clínicos e imagenológicos son los que sugieren el diagnóstico y permiten el adecuado seguimiento. Las diferentes modalidades diagnósticas como la ecografía, tomografía computarizada y resonancia magnética desempeñan un papel esencial en la identificación de las complicaciones de la ACF. El conocimiento de las diferentes manifestaciones radiológicas específicas de la enfermedad permitirá hacer un diagnóstico diferencial correcto con otras enfermedades hematológicas, un adecuado seguimiento de esta patología y un tratamiento precoz y oportuno. Con este artículo se pretende familiarizar al radiólogo con el espectro multisistémico de la ACF en la población pediátrica.

Introduction

Sickle cell anemia is an autosomal recessive disease characterized by abnormal hemoglobin formation that causes ischemic events and hemolysis, with multiple manifestations in imaging. It has a higher incidence in patients of African descent. Children are protected until 6 months of age by high levels of fetal hemoglobin (HbF). Its clinical presentation is variable; there may be recurrent painful crises, jaundice, short stature, strokes, and infections, mainly caused by encapsulated agents.

This article aims to familiarize radiologists with the imaging findings of multisystem manifestations in the pediatric population with sickle cell disease (SCD).

Etiology

Sickle cell disease, also known as sickle cell anemia, is a genetic disorder characterized by the production of abnormal hemoglobin, called hemoglobin S (HbS) (1). This defective hemoglobin causes red blood cells to take on a crescent shape, rather than the normal round and flexible shape, and leads to obstruction of blood flow, pain, organ damage, and stroke, among other things (2).

The etiology of SCD is due to a mutation in the *HBB* gene, which encodes the beta chain of hemoglobin. Specifically, there is a substitution of adenine for thymine in codon 6 of the *HBB* gene, causing a change from the amino acid glutamic acid to valine in the beta chain of hemoglobin. This mutation causes hemoglobin S to have a greater tendency to form polymers under conditions of low oxygenation, resulting in the deformation of red blood cells (3).

SCD is inherited in an autosomal recessive manner, meaning that a person needs to receive a copy of the mutated gene from each of their parents to develop the disease. If a person inherits only one copy of the mutated gene, they will be a carrier of the disease (sickle cell trait carrier), but will not normally have severe symptoms (4).

[1]Physician, Radiology resident, Universidad de Antioquia. Medellín, Colombia.

[2]Physician, radiologist, and professor, Universidad de Antioquia. Pediatric radiologist, Hospital Universitario San Vicente Fundación. Medellín, Colombia.

[3]Pediatric radiologist, Hospital Universitario San Vicente Fundación y Hospital Pablo Tobón Uribe. Medellín, Colombia.

[4]Physician, Radiology resident, Universidad CES. Medellín, Colombia. Institution: Department of Radiology at the Universidad de Antioquia.

Imaging manifestations

Infarctions are common throughout the body of patients with SCD, causing painful crises as a result of bone marrow infarcts (5). In the brain, infarcts of the white and gray matter are observed, causing cognitive impairment and neurological functional deficits (6). Patients may present with acute chest syndrome secondary to infarcts, embolisms—due to bone marrow infarcts and fat necrosis—and pulmonary infections (7). Abdominal organs may also suffer ischemic events. A rare but potentially fatal complication of SCD is sequestration syndrome, in which a considerable amount of intravascular volume becomes trapped in an organ (usually the spleen), causing vascular collapse (8). Finally, since the red blood cells are abnormal, they are removed from the circulation, leading to hemolytic anemia (9).

Different diagnostic modalities such as computed tomography (CT), magnetic resonance imaging (MRI), ultrasound, and conventional radiography are frequently used and indicated according to the organs or systems affected in patients with SCD. Table 1 summarizes the manifestations of SCD in different body systems.

Table 1. Manifestations of SCD by organs and systems

Organ/System	Manifestations
Multiorgan	Iron deposits Extramedullary hematopoiesis
Vascular	Vasculitis Vasculopathy
Central nervous system	Aneurysms Subarachnoid hemorrhage Stroke Cerebral atrophy Bone marrow hyperplasia in the skull
Musculoskeletal	Osteoporosis, osteomyelitis Osteonecrosis, septic arthritis H-shaped vertebrae Subperiosteal hemorrhages
Thorax	Pneumonia, embolism Chronic lung disease, infarcts
Hepatobiliary	Hepatomegaly, sequestration Hepatitis, cirrhosis Cholestasis, hepatocellular carcinoma Lithiasis Biliary stenosis
Spleen	Abscesses, sequestrations Infarcts, ruptures Auto-splenectomy
Gastrointestinal	Ulcers, pancreatitis Enterocolitis, intestinal ischemia
Renal	Infarctions, pyelonephritis Papillary necrosis, hemosiderosis Nephropathy
Genitals	Priapism Testicular atrophy

Manifestations in the central nervous system

Twenty-five percent of patients with SCD experience a neurological event in their lifetime (10). Most are asymptomatic, despite having imaging findings. When symptoms are present, they usually consist of varying degrees of cognitive impairment (11). Imaging findings are varied: ischemia and aneurysms with risk of secondary subarachnoid hemorrhage (Figures 1 and 2), tortuosity of arteries, stenosis, and cerebral atrophy (12). Moyamoya disease is a progressive, non-inflammatory, non-atherosclerotic occlusive vasculopathy characterized by a decrease in the caliber of the intracranial internal carotid arteries and proximal segments of the vessels of the circle of Willis, with proliferation of small abnormal vessels that give the characteristic "puff of smoke" appearance on panangiography (13) (Figures 3 and 4).

In a multicenter trial initiated in 1995 called the Stroke Prevention Trial in Sickle Cell Anemia (STOP), transcranial Doppler ultrasound (TCD) was used to stratify the risk of stroke in children with SCD. In this trial, the mean velocities of the middle cerebral arteries or internal carotid arteries were measured, and if all velocities were less than 170 cm/sec, the results were classified as normal. A velocity between 170 and 199 cm/sec was considered borderline, and a blood flow velocity >200 cm/sec was considered abnormal (14). To date, the STOP protocol continues to be implemented for the care of patients with SCD, which involves annual TCD screening for children between 2 and 16 years of age and more frequent follow-up for children with borderline or abnormal results. For patients identified as high risk due to velocities >200 cm/sec, the STOP protocol implements a chronic transfusion strategy to prevent stroke (15).

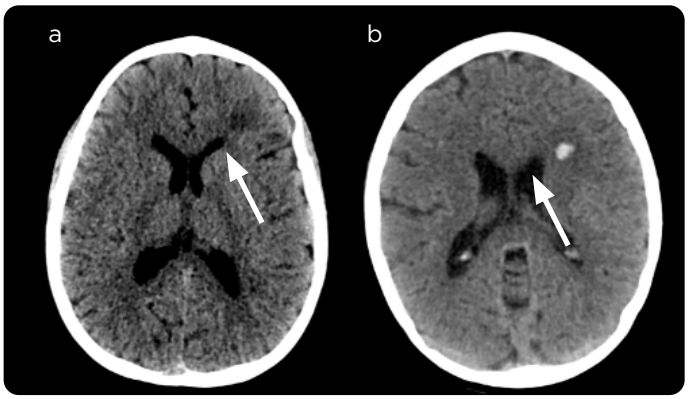


Figure 1. Male patient, 9 years old, with a history of SCD, who was admitted with ischemic stroke with right hemiparesis. a) Plain CT scan of the skull showing basal ganglia and b) lateral ventricles. Area of low density in the white matter in the left frontal region corresponding to ischemic changes. After 12 hours, high-density, rounded, intra-axial lesion measuring approximately 3 mm related to hemorrhagic transformation.

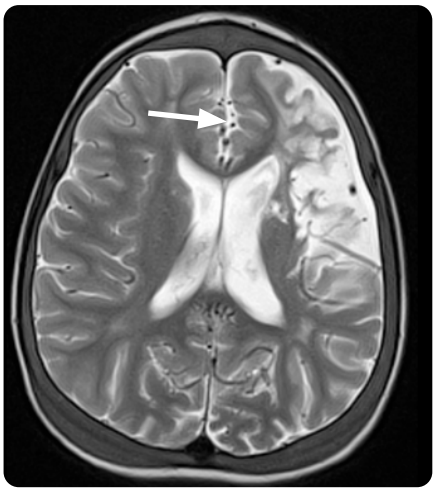


Figure 2. Male patient, 9 years old, with a history of SCD, who was admitted with ischemic stroke with right hemiparesis, attending a follow-up appointment two months later. Brain MRI, axial slice of lateral ventricles, T2 sequence. High signal in the left frontal lobe, corresponding to encephalomalacia and gliosis due to old infarction in the territory of the middle cerebral artery on the same side.

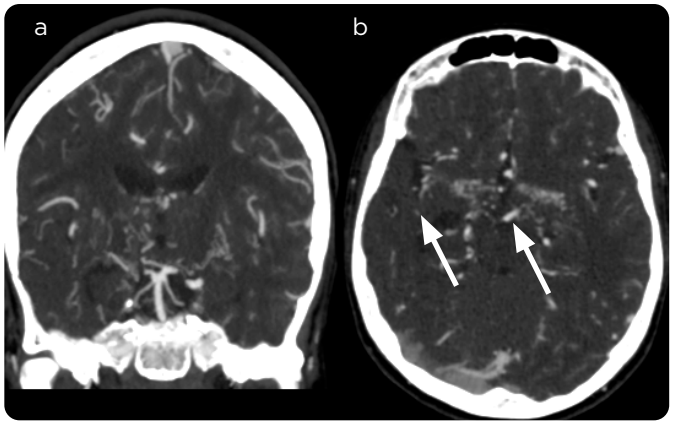


Figure 3. Male patient, 15 years old, history of SCD, presenting with brain target organ and subsequent development of moyamoya malformation. Contrast-enhanced CT scan of the skull. a) Coronal reconstruction and b) axial reconstruction of the basal ganglia. Decreased caliber of the intracranial internal carotid arteries and proximal segments of the vessels of the circle of Willis with development of lenticulo-striatal and thalamoperforating collaterals.

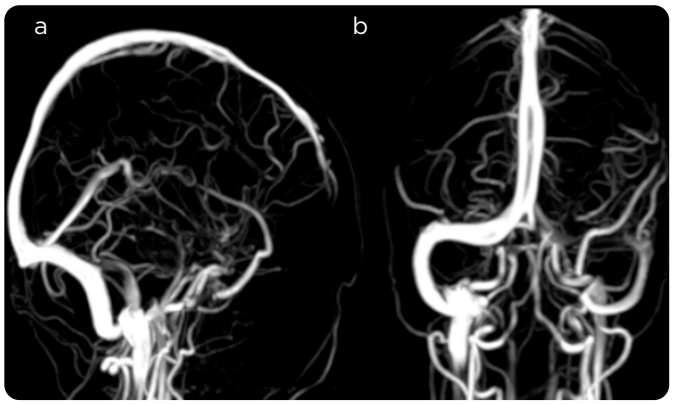


Figure 4. Male patient, 15 years old, history of SCD, presenting with brain as target organ and moyamoya malformation. Brain magnetic resonance angiography (ToF) MIP reconstructions. a) Sagittal and b) coronal. Multiple collaterals with stenosis of the anterior cerebral circulation, "smoke cloud" image due to moyamoya vessels.

Musculoskeletal manifestations

The skeletal manifestations of SCD are the result of three interrelated factors: vasocclusive episodes leading to bone infarcts and subperiosteal hemorrhages, chronic anemia causing expansion of the medullary spaces, and finally infections (16). These, in turn, can predispose individuals to other complications, such as bone development disorders and pathological fractures (17).

Bone marrow expansion also manifests as thinning of the inner and outer tables of the skull with expected thickening of the diploe (18). Osteoporosis of the cranial vault can produce a granular appearance on radiographs; vertical striations or "hair-like projections" that project from the posterior part (19) (Figure 5).

Acute soft head syndrome is a rare complication in children with SCD and is related to osteonecrosis and bone infarcts of the skull associated with secondary subgaleal collections that are managed conservatively (20) (Figure 6).

Infarctions of the terminal vertebral plates due to microvascular occlusion produce central depression, giving the appearance of an H-shaped vertebra (21) (Figure 7).

Bone infarction can occur anywhere in the skeleton and is caused by the sickle-shaped folding of red blood cells in the bone marrow, which leads to blood stasis, cell sequestration, hypoxia, and tissue ischemia, resulting in cell death (22). Infarctions typically occur in medullary cavities and epiphyses and are often the cause of painful bone crises, although they can also be silent and found incidentally in diagnostic imaging (23) (Figure 8).

Infarction and necrosis of the medullary bone create a breeding ground for the growth and spread of bacteria. The most common pathogens are Salmonella and S. aureus, among other Gram-negative bacteria (24). Osteomyelitis generally affects long bones, but it can also affect small bones, such as the vertebrae (Figure 9). Clinical manifestations include pain, edema, fever, and increased plasma inflammatory markers (25).

Distinguishing between osteomyelitis (OM) and bone infarcts from vasocclusive crises in children with SCD is difficult, particularly in the acute phase and in cases with negative cultures. In a study of pediatric patients with SCD who underwent musculoskeletal ultrasounds, it was found that in the group with osteomyelitis, 84% of cases presented with periosteal elevation and/or fluid accumulation. In the group of patients with vasocclusive crisis bone infarcts, the initial ultrasound showed no collections in 91% of cases, and when the ultrasound was repeated, none showed fluid accumulation (26). On contrast-enhanced MRI, the enhancement pattern can be useful in differentiating acute infarcts from OM. While bone infarcts show fine, peripheral enhancement, osteomyelitis shows more geographic and irregular enhancement of the marrow. Similarly, cases of osteomyelitis have shown cortical defects with abnormal signal intensities crossing the marrow to the soft tissues (22).

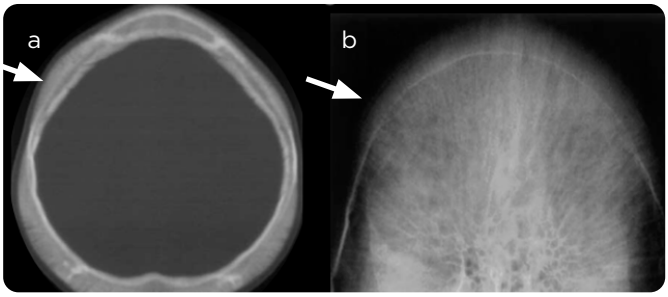


Figure 5. Female patient, 6 years old, history of SCD. a) Plain skull CT scan, axial section, bone window, and b) plain skull X-ray. Long, thin vertical streaks alongside thickening of the skull due to bone marrow hyperplasia ("hairy skull").

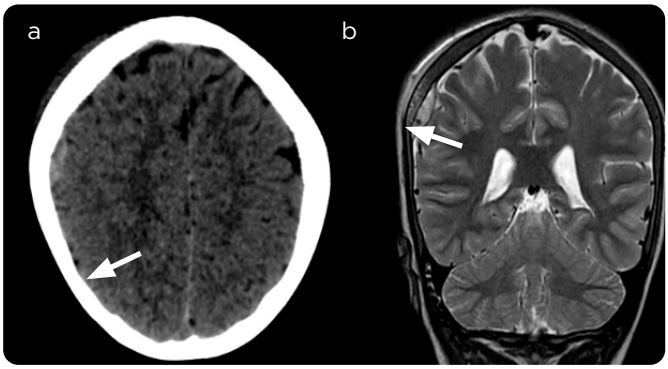


Figure 6. Male patient, 15 years old, hospitalized for painful crisis and headache. a) Plain CT scan of the skull showing the frontal lobes. High-density, lenticular-shaped extra-axial hemorrhage adjacent to the right frontal convexity, without mass effect, approximately 3 mm thick and associated with subgaleal collection. b) Brain MRI of the same patient, coronal T2 sequence. Bone infarction in the skull, subperiosteal hematoma, and laminar subgaleal collection.



Figure 7. Male patient, 14 years old, history of SCD. a) Lateral projection X-ray of the lumbar spine and b) sagittal plane CT scan of the thoracic spine. Flattening and collapse of the terminal vertebral plates, resulting in H-shaped vertebrae.

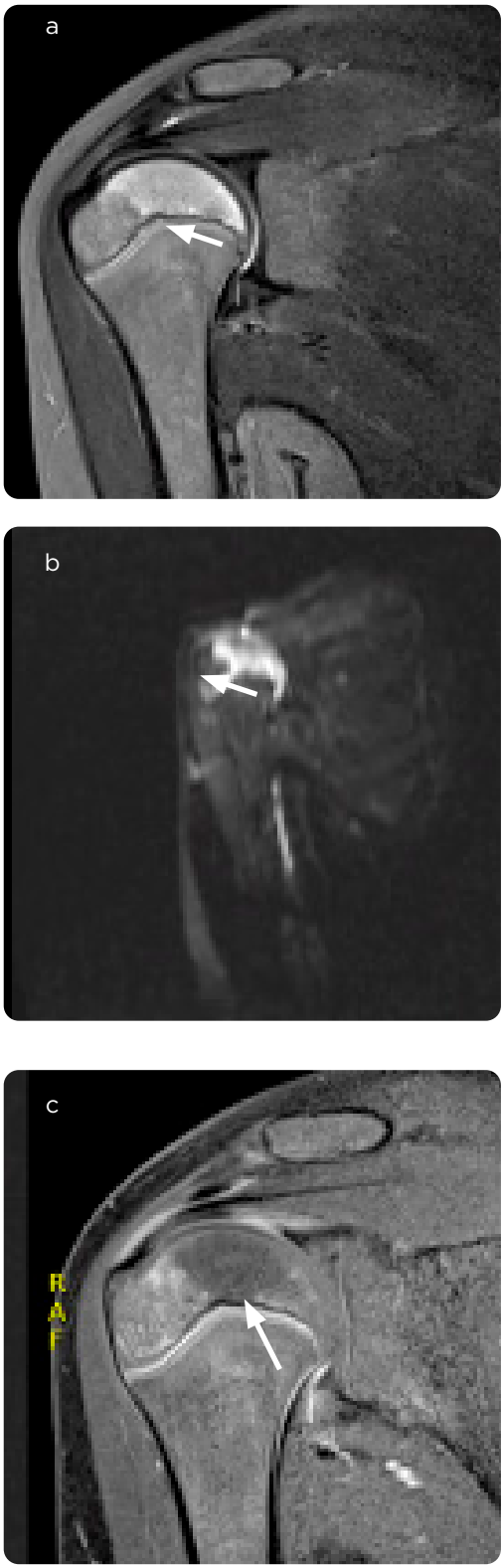


Figure 8. Female patient, 9 years old, history of SCD, attends the emergency department due to pain in her right upper limb. a) Shoulder MRI T2 sequences, b) diffusion, and c) T1 after contrast administration. Geographic area located in the proximal humeral epiphysis, surrounded by a line of low signal on T1 with high signal intensity on T2, without enhancement after contrast administration and diffusion restriction, characteristics suggestive of avascular necrosis of the humeral head.

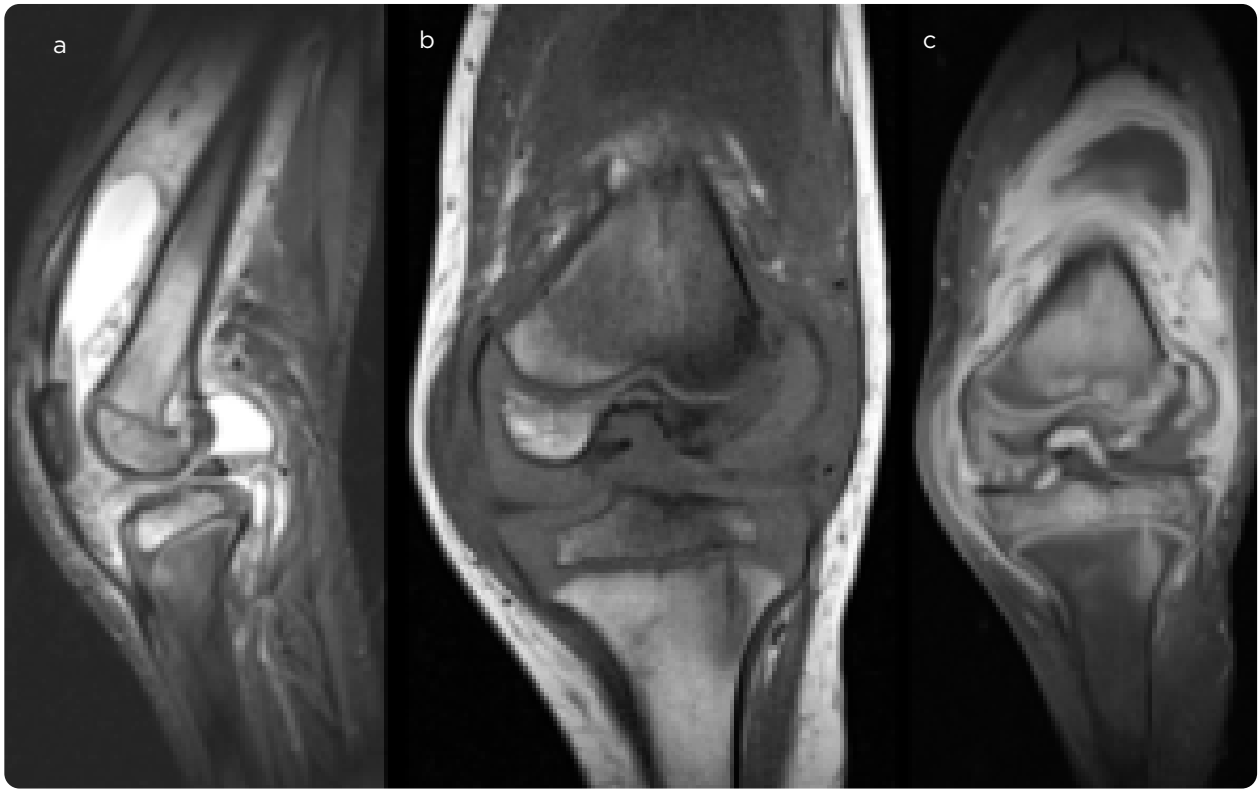


Figure 9. Male patient, 13 years old, history of SCD, now with pain and limitation in the right knee. Knee MRI, sagittal T2, coronal T1, and coronal T1 sequences after contrast administration. Diffuse enhancement of the thickened synovial membrane with accumulation of joint fluid. Abnormal, irregular, and poorly defined medullary edema, high signal on T2 and low signal on T1. A localized area of similar signal is observed in the medial femoral condyle, surrounded by a thin line of low T2/T1, with surrounding medullary edema and slight enhancement after contrast administration.

Thoracic manifestations

Acute chest syndrome

It is the most common cause of lung disease in these patients and is responsible for 25% of deaths. Episodes are recurrent in up to 80% of cases (27-30). It may be secondary to an infectious process, ischemia, or fat embolism. Children with CF are 100 times more likely to develop pneumonia than other children because their immune system is severely compromised (31, 32). Imaging findings generally include cardiomegaly secondary to chronic hypoxia, ground-glass opacities, and consolidations (Figures 10 and 11). Recurrence of this condition leads to pulmonary sequelae that can trigger fibrosis (33).

Abdominal manifestations

Abdominal manifestations of SCD are mainly secondary to vasocclusive crises, hemolysis, or infections. Cross-sectional imaging with ultrasound, CT, and MRI plays an essential role in identifying complications of the disease (34-36).

Sequestration occurs in 10%–30% of children aged 6–24 months and can often be fatal (37). Splenomegaly occurs in approximately 10% of patients over 10 years of age and is a consequence of vascular congestion (including sequestration), infarction, or abscess (37-39) (Figure 12). The clinical presentation includes sudden weakness or lethargy, tachycardia, abdominal pain, and pallor (40). Approximately 50% of children experience recurrent episodes (41). On ultrasound, the spleen appears as a heterogeneous parenchyma with multiple hypoechoic foci, and on CT, low peripheral density is the predominant finding. Splenic hemosiderosis is a phenomenon of chronic systemic iron overload with diffuse deposition of hemosiderin in reticuloendothelial tissues, including the spleen (42,43) (Figure 13).

Patients with SCD may develop renal dysfunction due to glomerulosclerosis and papillary necrosis. Ultrasound shows nephromegaly and increased medullary echogenicity (43-46) (Figure 14).

Renal medullary carcinoma is an aggressive cancer that occurs almost exclusively in patients with CKD, usually adolescent males (47). It manifests as a mass in the renal medulla, invading the renal sinus and cortex, often associated with dilation of the collecting system, peripheral extension, and adenopathy (48). On ultrasound, the mass is observed to have mixed echogenicity, with loss of corticomedullary differentiation and minimal or no flow on color Doppler ultrasound images (49) (Figure 15). On contrast-enhanced CT and MRI images, the tumor appears as an infiltrating, poorly defined, hypovascular, and heterogeneous mass, and the enhancement is usually less than that of the adjacent cortex and medulla (50) (Figure 16).

Right upper quadrant syndrome manifests as pain, jaundice, nausea, vomiting, painful hepatomegaly, and elevated transaminases and bilirubin; It is caused by stones, inflammation, cholestasis, hepatitis, and hepatotoxicity and can lead to chronic complications such as cirrhosis and subsequent liver fibrosis (51-53) (Figure 17).

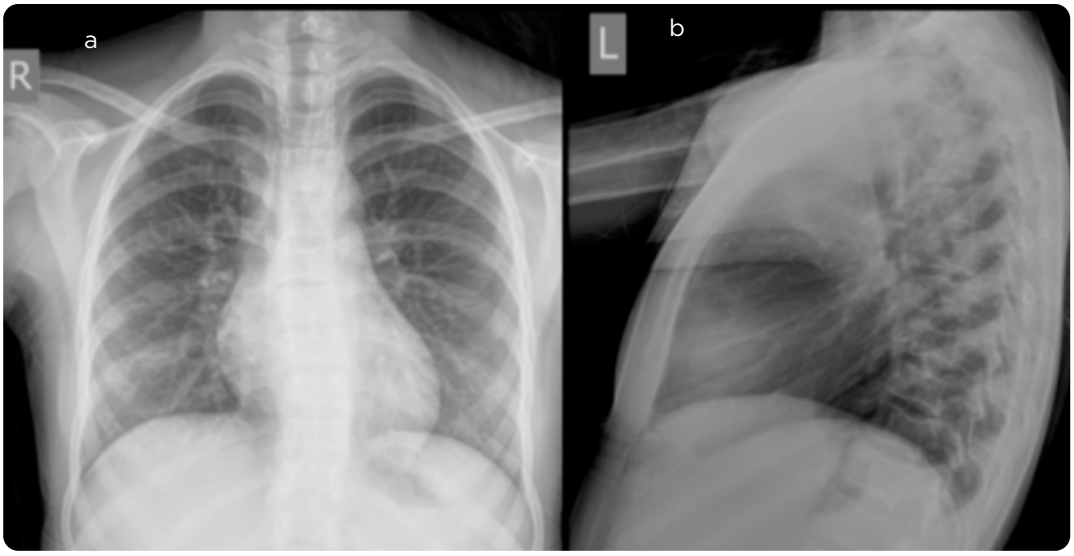


Figure 10. Female patient, 8 years old, dyspnea and chest pain. a and b) Chest X-ray. Posteroanterior and lateral projections showing bilateral basal alveolar glass opacities and H-shaped vertebrae.

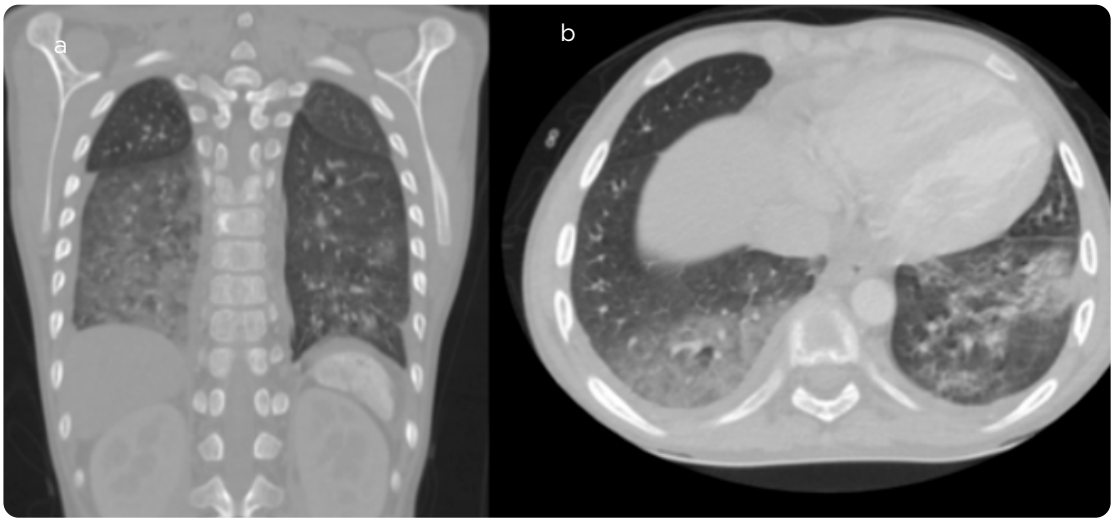


Figure 11. Female patient, 8 years old, with dyspnea and chest pain. Chest CT scan with contrast medium, a) coronal plane and b) axial plane. Ground-glass opacities and consolidations in both lower lobes due to pneumonia.

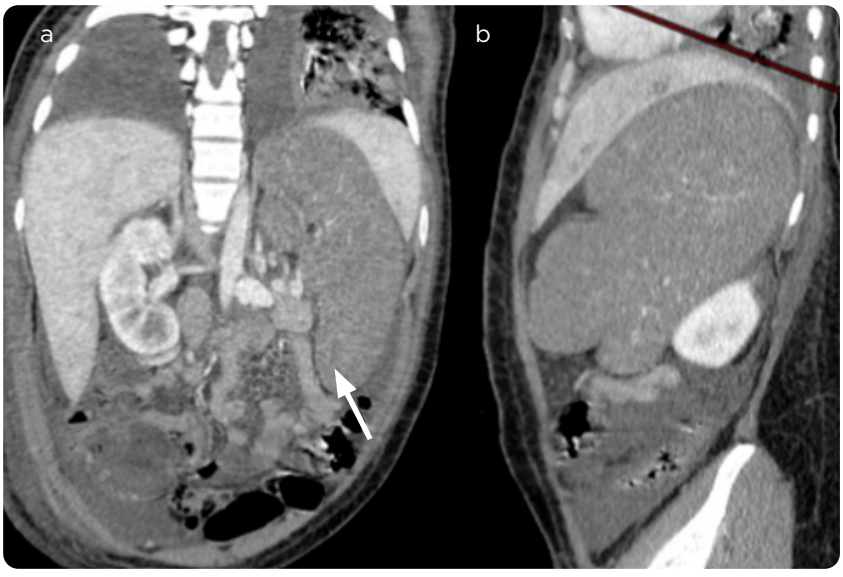


Figure 12. Male patient, 12 years old, history of SCD, with pain in the left hypochondrium for 8 days. Contrast-enhanced abdominal CT scan, a) coronal and b) sagittal. Enlarged spleen associated with low peripheral density, findings consistent with splenomegaly and splenic sequestration.

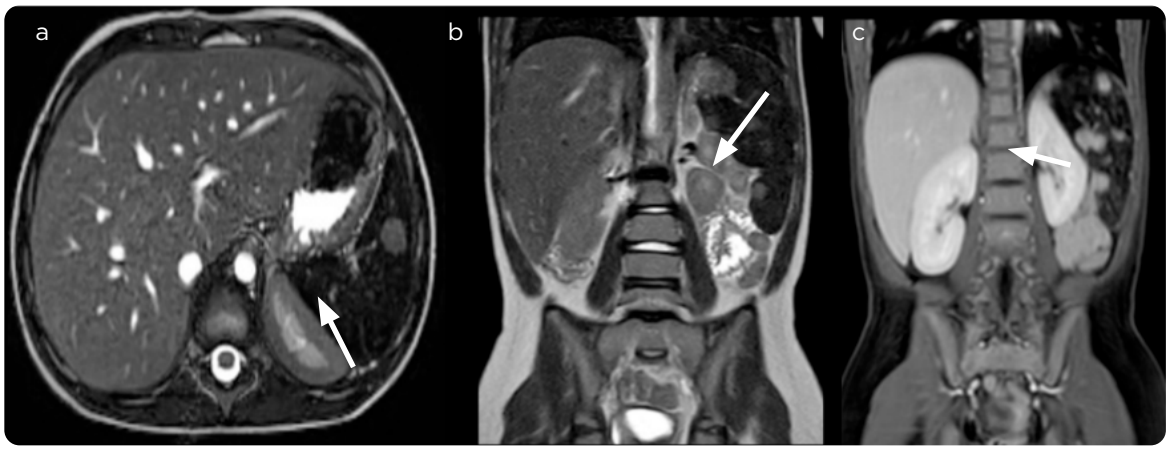


Figure 13. Male patient, 11 years old, history of SCD, now with abdominal pain. Abdominal MRI sequences a) axial T2, b) coronal T2, and c) T1. Low signal intensity in the spleen due to iron deposits with well-defined areas of high signal distributed throughout the parenchyma, corresponding to areas of respect.

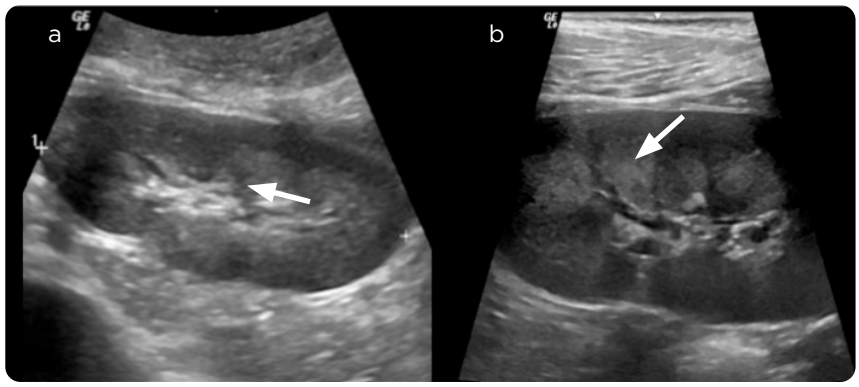


Figure 14. Female patient, 6 years old, history of SCD, ultrasound follow-up. Renal and urinary tract ultrasound. a and b) Increased echogenicity of the renal pyramids bilaterally due to vascular congestion.

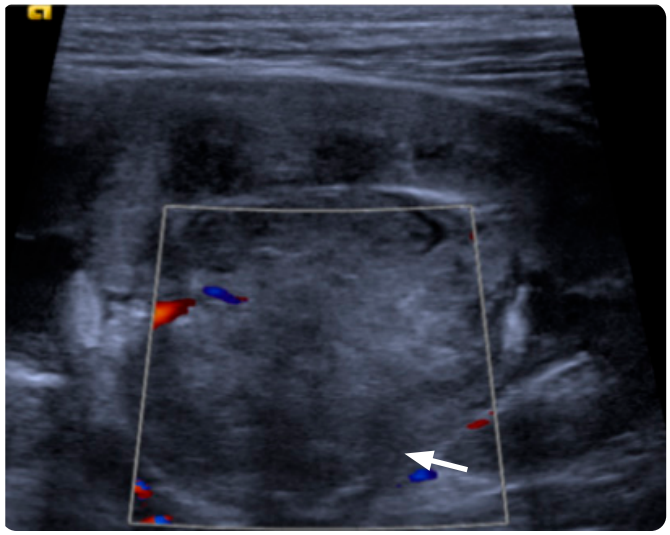


Figure 15. Female patient, 13 years old, history of SCD with recent diagnosis of renal medullary carcinoma. Renal and urinary tract ultrasound. Heterogeneous mass with poorly defined edges, located in the left renal sinus, without color Doppler signal, measuring approximately 5 cm in its largest diameter.

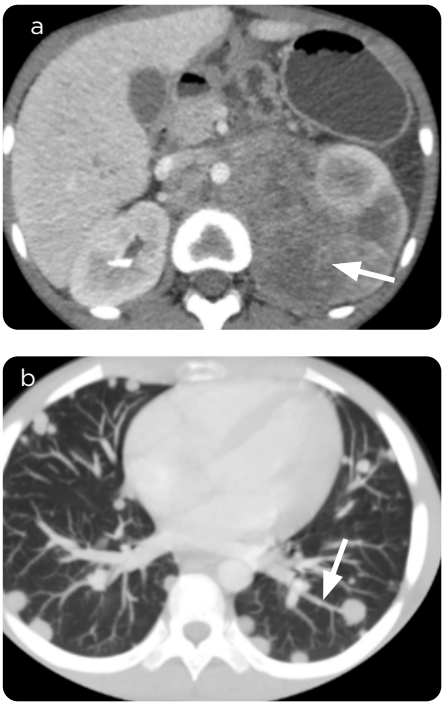


Figure 16. Female patient, 13 years old, history of SCD, recent diagnosis of renal medullary carcinoma and pulmonary metastasis. a) Contrast-enhanced abdominal CT scan: infiltrating mass of the left kidney, poorly defined, hypovascular, and heterogeneous with lower enhancement than the adjacent cortex and medulla. b) Contrast-enhanced chest CT scan: multiple solid nodules of random distribution and variable size due to metastasis. Associated inflammatory lesions.

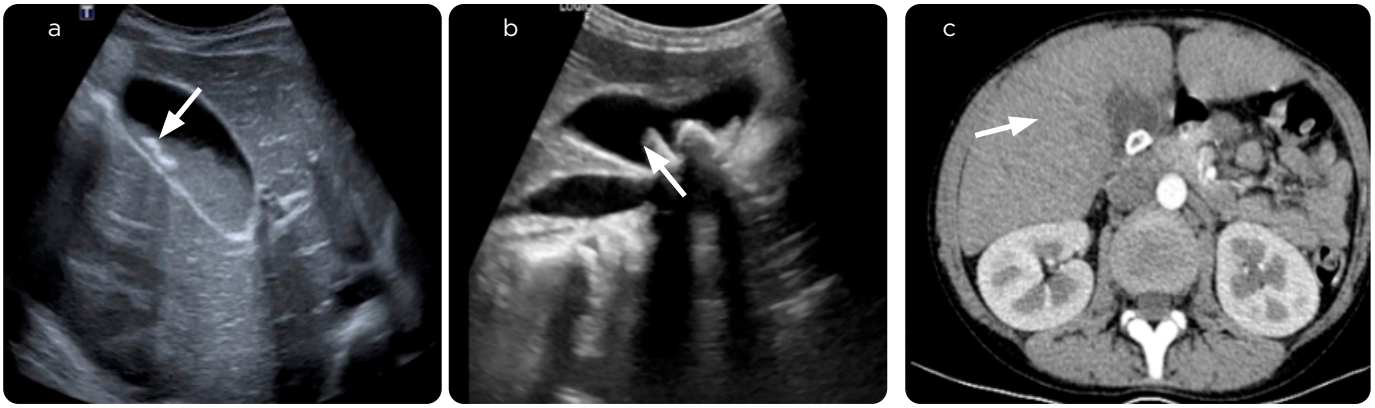


Figure 17. Male patient, 10 years old, with colicky abdominal pain located in the right hypochondrium. a and b) Total abdominal ultrasound showing amorphous, mobile echoes without acoustic shadowing, located in the gallbladder, in areas of decline, consistent with biliary sludge, associated with multiple echogenic, mobile images that cast posterior acoustic shadowing consistent with stones, without additional inflammatory signs; findings consistent with cholelithiasis without cholecystitis. c) Contrast-enhanced abdominal CT scan in the portal phase. Gallstone in the gallbladder, without signs.

Conclusions

Diagnostic imaging plays an essential role in the management of pediatric patients with sickle cell anemia. Knowledge of the different imaging manifestations of the disease will enable a correct differential diagnosis with other diseases, adequate monitoring of this pathology, and facilitate early and timely treatment.

References

1. Pinto VM, Balocco M, Quintino S, Forni GL. Sickle cell disease: a review for the internist. Intern Emerg Med. 2019;14(7):1051-64.
2. Piel FB, Steinberg MH, Rees DC. Sickle cell disease. N Engl J Med. 2017;376(16):1561-73.
3. Azar S, Wong TE. Sickle cell disease: a brief update. Med Clin North Am. 2017;101(2):375-93.
4. Taher AT, Weatherall DJ, Cappellini MD. Thalassaemia. Lancet. 2018;391(10116):155-67.
5. Steinberg MH. Sickle cell anemia, the first molecular disease: overview of molecular etiology, pathophysiology, and therapeutic approaches. Scientific World J. 2008;8:1295-324.
6. Nemzek WR, Swartz JD. Temporal bone: inflam matory disease. En: Som PM, Curtin HD, eds. Head and neck imaging. 4th ed. St. Louis, Mo: Mosby, 2003; pp. 1207-8.
7. Gladwin MT, Vichinsky E. Pulmonary complications of sickle cell disease. N Engl J Med. 2008;359:2254.
8. Joseph E. Maakaron, Chief Editor: Emmanuel C Besa, Sickle Cell Anemia Clinical presentation. http://www.ncbi.nlm.nih.gov/pubmed/216513. Updated: Jan 28, 2013.
9. Rees DC, Williams TN, Gladwin MT. Sickle-cell disease. Lancet. 2010;376(9757):2018-31.
10. Saito N, Nadgir RN, Flower EN, Sakai O. Clinical and radiologic manifestations of sickle cell disease in the head and neck. Radiographics. 2010;30(4):1021-34. http://dx.doi.org/10.1148/rg.304095171 .
11. Kotb MM, Tantawi WH, Elsayed AA, Damanhouri GA, Malibary HM. Brain MRI and CT findings in sickle cell disease patients from Western Saudi Arabia. Neurosciences (Riyadh). 2006;11(1):28-36. PMID: 22266500.
12. Thust SC, Burke C, Siddiqui A. Neuroimaging findings in sickle cell disease. Br J Radiol. 2014;87(1040):20130699. https://doi.org/10.1259/bjr.20130699. Epub 2014 May 21.
13. Allison JW, Glasier CM, Stark JE, James CA, Angtuaco EJ. Head and neck MR angiography in pediatric patients: a pictorial essay. Radiographics. 1994;14(4):795-805.
14. Adams R, McKie V, Hsu L, et al. Prevention of a first stroke by transfusion in children with abnormal results of transcranial Doppler ultrasonography. N Engl J Med. 1998;339:5-11.
15. Guy D, Bagnall R, Morgan RL, Babatunde I, Nevière A, Friedrich G, et al. Impact of transcranial Doppler screening on stroke prevention in children and adolescents with sickle cell disease: A systematic review and meta-analysis. Blood Rev. 2024; 12:101253. https://doi.org/10.1016/j.blre.2024.101253.
16. Ochocinski D, Dalal M, Black LV, et al. Life-threatening infectious complications in sickle cell disease: a concise narrative review. Front Pediatr. 2020;8:38.
17. Ginzel AW, Kransdorf MJ, Peterson JJ, Garner HW, Murphey MD. Mass-like extra medullary hematopoiesis: imaging features. Skeletal Radiol. 2012;41:911-6.
18. Reed Kearney P, Nasser A. Pathology quiz case 2: extramedullary hematopoeisis (EMH) of para nasal sinuses. Arch Otolaryngol Head Neck Surg. 2002;128(1):76-9.
19. Berkmen Yahya M, Zalta Benjamin A. Case 126: extramedullary hematopoiesis. Radiology. 2007;245(3):905-8. http://dx.doi.org/10.1148/radiol.2453040715.
20. Zadeh C, Rameh V, Atweh LA. Acute soft head syndrome in a sickle cell disease patient. J Radiol Case Rep. 2021;15(4):1-6. https://doi.org/10.3941/jrcr.v15i4.4026.
21. Almeida A, Roberts I. Bone involvement in sickle cell disease. Br J Haematol. 2005;129:482-90.
22. Umans H, Haramati N, Flusser G. The diagnostic role of gadolinium enhanced MRI in distinguishing between acute medullary bone infarct and osteomyelitis. Magn Reson Imaging. 2000;18:255-62.
23. Collett-Solberg PF, Ware RE, O'Hara SM. Asymmetrical closure of epiphyses in a patient with sickle cell anemia. J Pediatr Endocrinol Metab. 2002;15:1207-12.
24. Desimpel J, Posadzy M, Vanhoenacker F. The many faces of osteomyelitis: a pictorial review. J Belg Soc Radiol. 2017;101(1):24.
25. Ejindu VC, Hine AL, Mashayekhi M, Shorvon PJ, Misra RR. Musculoskeletal manifestations of sickle cell disease. RadioGraphics. 2007;27(4):1005-21.
26. Inusa BP, Oyewo A, Brokke F, Santhikumaran G, Jogeesvaran KH. Dilemma in differentiating between acute osteomyelitis and bone infarction in children with sickle cell disease: the role of ultrasound. PLoS One. 2013;8(6):e65001. https://doi.org/10.1371/journal.pone.0065001.
27. Melton CW, Haynes J Jr. Sickle acute lung injury: role of prevention and early aggressive intervention strategies on outcome. Clin Chest Med. 2006;27(3):487-502, vii.
28. Machado RF, Gladwin MT. Chronic sickle cell lung disease: new insights into the diagnosis, pathogenesis and treatment of pulmonary hypertension. Br J Haematol. 2005;129:449-64.
29. Godeau B, Schaeffer A, Bachir D, Fleury-Feith J, Galacteros F, Verra F, et al. Bronchoalveolar lavage in adult sickle cell patients with acute chest syndrome: value for diagnostic assessment of fat embolism. Am J Respir Crit Care Med. 1996;153(5):1691-6.
30. Miller AC, Gladwin MT. Pulmonary complications of sickle cell disease. Am J Respir Crit Care Med. 2012;185:1154-65.
31. Kang J, Litmanovich D, Bankier AA, et al. Manifestations of systemic diseases on thoracic imaging. Curr Probl Diagn Radiol. 2010;39:247-61.
32. Mekki F, Taktak S, Khaldi H, et al. Acute chest syndrome as the inaugural sign of sickle cell anemia. A case report and review of the literature. Rev Pneumol Clin. 2006;62:195-9.
33. Vij R, Machado RF. Pulmonary complications of hemoglobinopathies. Chest. 2010;138(4):973-83. https://doi.org/10.1378/chest.10-0317.
34. Gardner CS, Boll DT, Bhosale P, Jaffe TA. CT abdominal imaging findings in patients with sickle cell disease: acute vaso-occlusive crisis, complications, and chronic sequelae. Abdom Radiol (NY). 2016;41(12):2524-32.
35. Kinger NP, Moreno CC, Miller FH, Mittal PK. Abdominal manifestations of sickle cell disease. Curr Probl Diagn Radiol. 2021;50(2):241-51.

36. Solomon N, Segaran N, Badawy M, Elsayes KM, Pellerito JS, Katz DS, et al. Manifestations of sickle cell disorder at abdominal and pelvic imaging. Radiographics. 2022;42(4):1103-22.
37. Sheth S, Ruzal-Shapiro C, Piomelli S, Berdon WE. CT imaging of splenic sequestration in sickle cell disease. Pediatr Radiol. 2000;30(12):830-3.
38. Jefferson JM, Sims WM, Umeh N, Byeon YJJ, Abdallah KE, Bonham VL, et al. Splenic infarction in sickle cell trait: A comprehensive systematic review of case studies. EJHaem. 2021;2(3):585-600.
39. Al-Salem AH. Splenic complications of sickle cell anemia and the role of splenectomy. ISRN Hematol. 2011;2011:864257.
40. Brousse V, Buffet P, Rees D. The spleen and sickle cell disease: the sick(led) spleen. Br J Haematol. 2014;166(2):165-76.
41. Tennenbaum J, Volle G, Buffet P, Ranque B, Pouchot J, Arlet JB. Dysfonction splénique au cours de la drépanocytose : mise au point [Splenic dysfunction in sickle cell disease: An update]. Rev Med Interne. 2023;44(7):335-43. French.
42. Consul N, Javed-Tayyab S, Morani AC, Menias CO, Lubner MG, Elsayes KM. Iron-containing pathologies of the spleen: magnetic resonance imaging features with pathologic correlation. Abdom Radiol (NY). 2021;46(3):1016-26.
43. Thomas AJ, Morani AC, Liu PS, Weadock WJ, Hussain HK, Elsayes KM. Iron-containing abdominal pathologies: exploiting magnetic susceptibility artifact on dual-echo gradient-echo magnetic resonance imaging. J Comput Assist Tomogr. 2019;43(2):165-75.
44. Patel R, Kang S, Valeshabad AK, et al. Kidney ultrasound findings according to kidney function in sickle cell anemia. Am J Hematol. 2019;94(11):E288-91.
45. Jung DC, Kim SH, Jung SI, Hwang SI, Kim SH. Renal papillary necrosis: review and comparison of findings at multi-detector row CT and intravenous urography. RadioGraphics. 2006;26(6):1827-36.
46. Purysko AS, Westphalen AC, Remer EM, Coppa CP, Leão Filho HM, Herts BR. Imaging manifestations of hemato logic diseases with renal and perinephric involvement. RadioGraphics. 2016;36(4):1038-54.
47. Ruiz MA, Zhang X, Mansilla MA, Zahr RS, Thomas CP, Smith RJ, et al. Prevalence of kidney health genetic variants in adults with sickle cell nephropathy. Br J Haematol. 2024;205(1):316-9.
48. Raman SP, Hruban RH, Fishman EK. Beyond renal cell carcinoma: rare and unusual renal masses. Abdom Imaging. 2012;37(5):873-84.
49. Blitman NM, Berkenblit RG, Rozenblit AM, Levin TL. Renal medullary carcinoma: CT and MRI features. AJR Am J Roentgenol. 2005;185(1):268-72.
50. Khan A, Thomas N, Costello B, et al. Renal medullary carcinoma: sonographic, computed tomography, magnetic resonance and angiographic findings. Eur J Radiol. 2000;35(1):1.
51. Greco F, Faiella E, Santucci D, et al. Imaging of renal medullary carcinoma. J Kidney Cancer VHL. 2017;4(1):1-7.
52. Theocharidou E, Suddle AR. The liver in sickle cell disease. Clin Liver Dis. 2019;23(2):177-89.
53. Martins RA, Soares RS, Vito FB, et al. Cholelithiasis and its complications in sickle cell disease in a university hospital. Rev Bras Hematol Hemoter. 2017;39(1):28-31.

Correspondence

María Isabel González Gómez
Carrera 51D # 62-29, La Candelaria
Medellín, Antioquia
maria.gonzalez8@udea.edu.co

Received for evaluation: January 25, 2024
Accepted for publication: January 30, 2024